

Sensor-Based Gait Analysis: A Comparative Study of Ultrasonic and Laser Sensors for Gait Monitoring in Rollator-Assisted Walking

Ivan Omeko, Stefan Twieg and Martin Obert

¹*Department of Electrical, Mechanical and Industrial Engineering, Anhalt University of Applied Sciences, Bernburger Str. 55, Köthen, Germany*

Ivan.Omeko@student.hs-anhalt.de, Stefan.Twieg@hs-anhalt.de, Martin.Obert@hs-anhalt.de

Keywords: Sensor, Signal Processing, Gait Analysis, Ultrasonic Sensor, Laser Sensor, Machine Learning, Algorithms, Elderly Support, Rollator.

Abstract: The AktiMuW project aims to enhance mobility assistance for elderly individuals by developing a smart rollator equipped with advanced posture monitoring. A crucial aspect of this system is the detection and correction of the user's posture of legs. This is based on measuring the distance between the user and the rollator, among other methods. The study evaluates three different distance sensors – HC-SR04, HC-SR04-P, and TFmini-S to determine the most reliable and suitable option. To achieve this, a series of use case centered experiments were conducted, where each sensor's performance was tested. The HC-SR04 demonstrated relatively low measurement error, with Root Mean Square Error (RMSE) values ranging from 0.64 cm to 0.89 cm but required a 5V power supply and additional voltage conversion components, complicating integration to single board computers (SBC). The HC-SR04-P, an updated model, operates reliably at 3.3V – compatible with Raspberry Pi boards – and maintained comparable measurement precision, with RMSE values of 0.57 cm and 0.78 cm. In contrast, the TFmini-S LiDAR sensor exhibited higher RMSE values of 5.42 cm and 2.89 cm, particularly struggling at shorter distances, making it unsuitable for this application. Further gait analysis tests confirmed that the HC-SR04-P could effectively monitor the user's position, despite occasional signal reflections. The study concludes that the HC-SR04-P is the optimal choice for the rollator Machine Learning algorithms due to its balance of accuracy, compatibility, and cost-effectiveness. These findings contribute to the theoretical understanding of sensor-based posture monitoring and hold practical significance for the development of assistive mobility devices and further algorithms.

1 INTRODUCTION

1.1 Motivation

As people age, they often require more assistance [1]. According to [2], mobility declines significantly with age, as majority of people over 85 experience some difficulty walking, and mobility disability is linked to increased risks of social isolation, falls, and depression. Robotics can help provide essential support to enhance their independence and quality of life [3]. The goal of the AktiMuW [4] project is to develop a smart rollator for elderly individuals, providing them with enhanced assistance [5] in daily tasks, whether navigating indoors or walking to the nearest grocery store (for instance, with the help of road signs detection [6]).

One key area of development in the project is posture monitoring, which relies on data from

multiple sensors. To achieve accurate posture assessment, it is crucial to identify the most suitable sensor for measuring the distance between the AktiMuW Rollator and the user for gait identification [7], [8]. The following tests aim to determine which sensor best fulfills this role.

1.2 Problem Statement

Ultrasonic sensors HC-SR04 [9] are widely used for various applications. These ultrasonic sensors have been implemented to measure the distance between the rollator and the user's legs but have demonstrated inconsistent performance. This leads to reliability issues for addressed use case of gait analysis. To address this challenge, a study based on a series of tests was conducted to evaluate sensor technology and determine the most suitable option for the project.

The main technical focus is set to compare ultrasonic versus laser sensor. By analyzing the

performance of pre-selected sensors, the goal is to identify the most effective solution for accurately measuring the user's distance from the rollator. The findings from these tests will lead to further improvements in the smart rollator's design, particularly in enhancing its posture detection machine learning algorithms [10], [11], [12], [13].

2 SENSORS REVIEW

The evaluation process involved comparing three different sensor types:

- HC-SR04 (5V),
- HC-SR04-P (3.3V),
- TFmini-S (5V).

The current study setup for distance reading consists of Raspberry Pi Zero W with, for instance, two ultrasonic sensors HC-SR04, like shown in Figure 1.

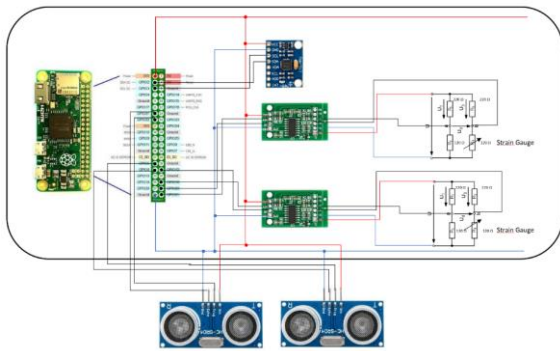


Figure 1: Raspberry Pi Zero W Schematic of Sensor Connections.

2.1 HC-SR04

HC-SR04, shown in Figure 2, is the ultrasonic sensor that was used for first proof of concept implementation on rollator.

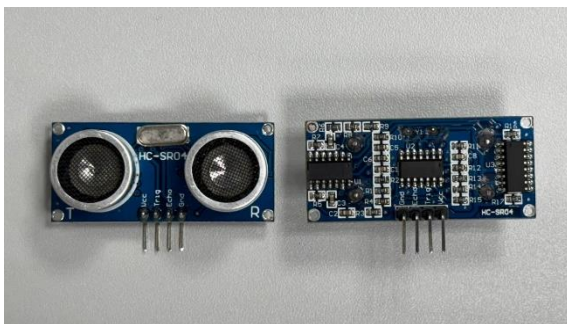


Figure 2: HC-SR04 ultrasonic sensor.

Characteristics are:

- Working Voltage: DC 5V;
- Working Current: 15 mA;
- Working Frequency: 40 Hz;
- Maximum Range: 4 m;
- Minimum Range: 2 cm;
- Measuring Angle: 15 degrees;
- Dimensions: 45x20x15 mm;
- Price: approx. 3€.

Reviewing the device specifications and connection schematics reveals that the HC-SR04 sensor needs to be powered by 5V. GPIO of Raspberry Pi Zero board requires 3.3V, but supports 5V power supply. This mismatch causes issues with the Raspberry Pi.

However, the main problem is that sensor does not perform voltage conversion on its ECHO pin, while the Raspberry Pi's GPIO can only handle 3.3V. As a solution, a voltage divider consisting of two resistors can be used. With all this in mind, electrical connection scheme is shown in Figure 3.

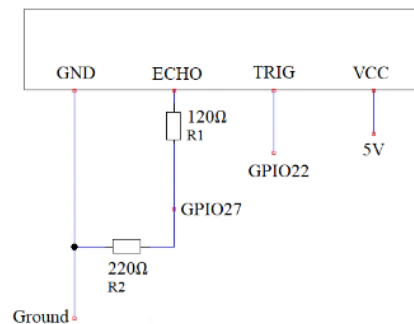


Figure 3: Scheme of HC-SR04 connected to Raspberry Pi powered by 5V and voltage divider at ECHO pin.

2.2 HC-SR04-P

Figure 4 displays HC-SR04-P [14], which is a version of HC-SR04 sensor that can operate both at 5V and 3.3V.

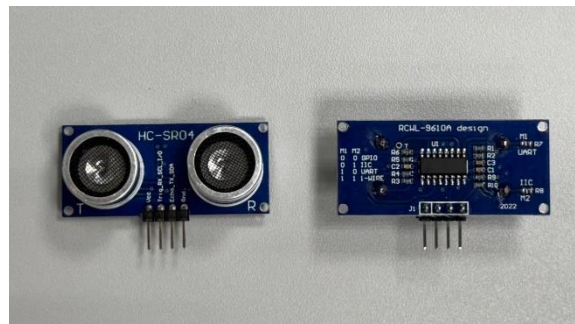


Figure 4: HC-SR04-P ultrasonic sensor.

Characteristics are:

- Working Voltage: DC 3.3–5V;
- Working Current: <2 mA;
- Working Frequency: 40 Hz;
- Maximum Range: 500 cm;
- Minimum Range: 2 cm;
- Measuring Angle: 15 degrees;
- Dimensions: 45x20x15 mm;
- Price: approx. 3€.

Since the HC-SR04-P is merely a modification of the HC-SR04, the main advantage is, that this sensor will be directly connected with 3.3V power and GPIO. Within following evaluation, it is analyzed if performance differs between 5V and 3.3V version.

2.3 TFmini-S

The TFmini-S [15] is a single-point LiDAR sensor. It was included in the tests to introduce a different type of sensor, distinct from ultrasonic sensors, and to compare their performance. Figure 5 illustrates the visual appearance of the sensor.

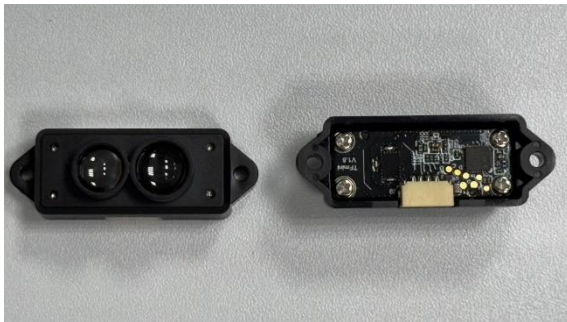


Figure 5: TFmini-S single-point LiDAR sensor.

Its characteristics are as follows:

- Operating range: 0.1m–12m;
- Accuracy: ±6 cm at 0.1–6m, ±1% at 6m–12m;
- Measurement unit: cm;
- Range resolution: 1cm;
- FOV: 2 degrees;
- Frame rate: 1~1000Hz;
- Supply voltage: 5V±0.1V;
- Average current: ≤140mA;
- Peak current: 200mA;
- Average power: 700mW;
- Communication level: LVTTL (3.3V);
- Price: approx. 42€.

3 PRE-EVALUATION ANALYSIS

3.1 Sensor Test Setup

Each sensor will be tested individually by detecting an obstacle at four distances: 5 cm, 30 cm, 60 cm, and 100 cm. The boundaries of 5 cm and 100 cm were chosen because rollator users are likely to operate within this range. The goal is to evaluate the accuracy of each sensor type and compare their performance, like shown in Figure 6.

To provide a compact measure of each sensor's performance, tables, such as Table 2, present the average distance measurements recorded by each sensor at four test distances. These averages offer a simplified view of each sensor's typical response at each range.

The bottom row of the table reports the Root Mean Square Error (RMSE) [16] for each sensor, calculated relative to the true distances. RMSE is computed from the average readings and provides a single-value summary of overall deviation. It is defined as:

$$RMSE = \sqrt{\frac{1}{n} \sum_{i=1}^n (measured_i - actual_i)^2} \quad (1)$$

where n is the number of test distances.

The test setup consists of:

- Raspberry Pi Zero W,
- Laptop with SSH connection to the Raspberry Pi,
- USB-A to Micro-USB cable,
- a breadboard,
- jumper cables,
- 120Ω and 220Ω resistors,
- Measuring tape fixed to a desk,
- Centered cardboard box as an obstacle.



Figure 6: Example of the test setup. HC-SR04 tested at 30 cm.

3.2 HC-SR04 Test

As mentioned before, HC-SR04 will be powered by 5V with connected and voltage divider at ECHO pin, consisting of 120Ω and 220Ω resistors.

Connections between the HC-SR04 and the Raspberry Pi Zero W are shown in Table 1.

Table 1: Connections between two HC-SR04 or HC-SR04-P and the Raspberry Pi Zero W.

HC-SR04 (-P) Left	Raspberry Pi Zero W	HC-SR04 (-P) Right	Raspberry Pi Zero W
VCC	5V/ 3V3	VCC	5V/ 3V3
TRIG	GPIO22	TRIG	GPIO5
ECHO	GPIO27	ECHO	GPIO6
GND	Ground	GND	Ground

Figures 7 - 10 show the results of conducted tests with HC-SR04 sensors.

Table 2: Average distance readings for each HC-SR04 unit.

Test Distance, cm	Average readings, cm			
	HC-SR04 1	HC-SR04 2	HC-SR04 3	HC-SR04 4
5	5.39	5.20	5.54	5.42
30	30.52	30.12	30.88	30.30
60	59.95	59.55	59.70	60.15
100	98.73	98.40	98.97	98.87
RMSE, cm	0.74	0.89	0.79	0.64

As shown in Figures 7–10 and Table 2, all four sensor units generally provide consistent distance measurements to the object in front of them. However, occasional outliers to random distances occur. Notably, these outliers appear on different sensors at various distances, suggesting they may be caused by external interference.

The Root Mean Square Error for individual sensors ranges from 0.64 cm to 0.89 cm, reflecting relatively small overall deviations from the true values.

3.3 HC-SR04-P Test

Since HC-SR04-P is just a modification of HC-SR04 that can operate at both 5V and 3.3V, in this test for variability it will be powered by 3.3V without voltage divider at ECHO pin. Additionally, the current Raspberry Pi setup on the rollator already powers the ultrasonic sensors via 3.3V. Connections are shown in Table 1. Figures 11–14 show the results of conducted tests with HC-SR04-P.

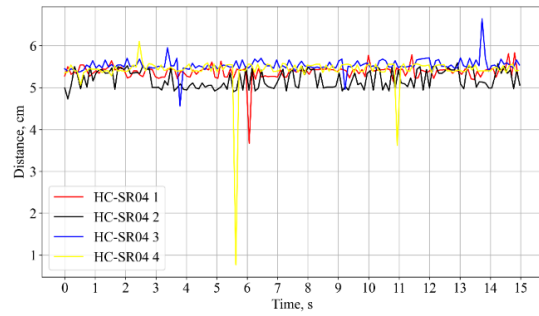


Figure 7: Comparison of four HC-SR04 units at 5 cm.

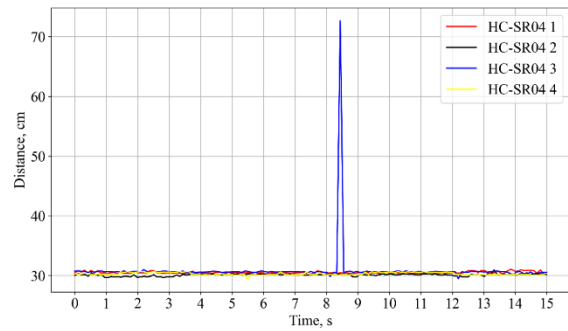


Figure 8: Comparison of four HC-SR04 units at 30 cm.

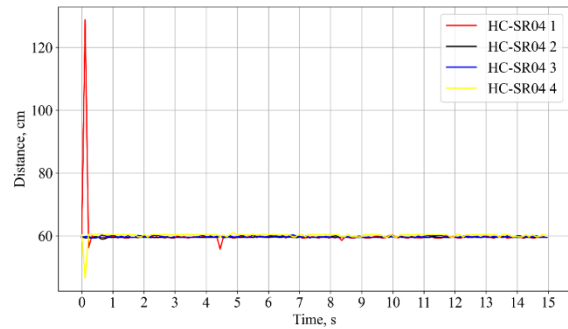


Figure 9: Comparison of four HC-SR04 units at 60 cm.

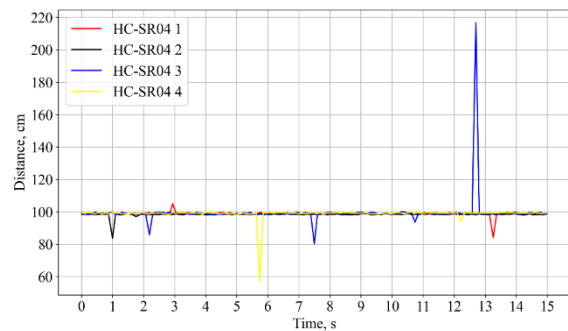


Figure 10: Comparison of four HC-SR04 units at 100 cm.

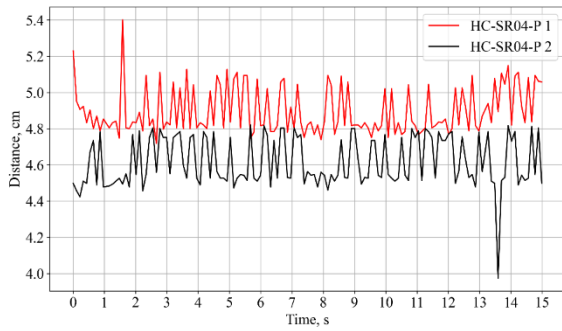


Figure 11: Comparison of two HC-SR04-P units at 5 cm.

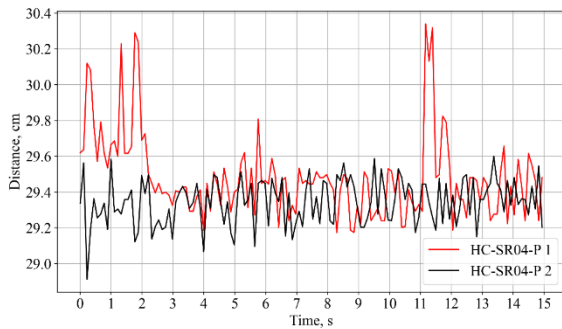


Figure 12: Comparison of two HC-SR04-P units at 30 cm.

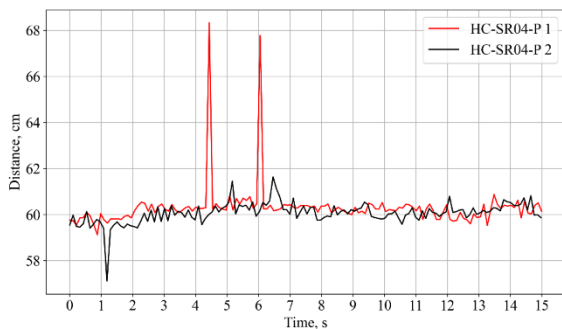


Figure 13: Comparison of two HC-SR04-P units at 60 cm.

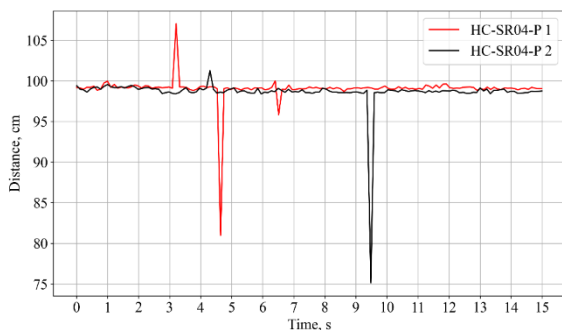


Figure 14: Comparison of two HC-SR04-P units at 100 cm.

Table 3: Average distance readings for each HC-SR04-P unit.

Test Distance, cm	Average readings, cm	
	HC-SR04-P 1	HC-SR04-P 2
5	4.90	4.62
30	29.47	29.35
60	60.30	60.07
100	99.05	98.63
RMSE, cm	0.57	0.78

It can be observed from Table 3 that the HC-SR04-P is very similar to the HC-SR04 in terms of accuracy. However, it appears to be less prone to sudden outliers in readings.

The Root Mean Square Error is 0.57 cm and 0.78 cm for the first and second units, respectively, indicating high accuracy relatively to the actual test distances.

3.4 TFmini-S Test

Connections between the TFmini-S and the Raspberry Pi are shown below in Table 4.

Table 4: Connections between the TFmini-S and the Raspberry Pi Zero W.

TFmini-S	Raspberry Pi
5V(RED)	5V
GND(BLACK)	Ground
RX(WHITE)	TXD0
TX(GREEN)	RXD0

Results of testing are shown in Figures 15 to 18.

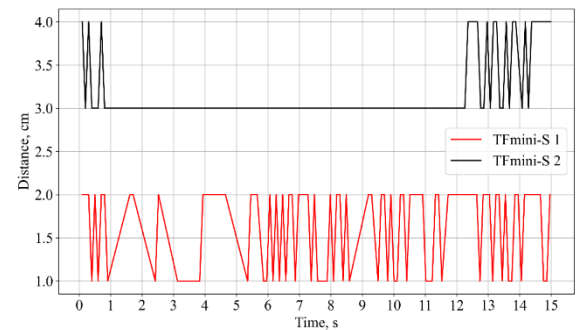


Figure 15: Comparison of two TFmini-S units at 5 cm.

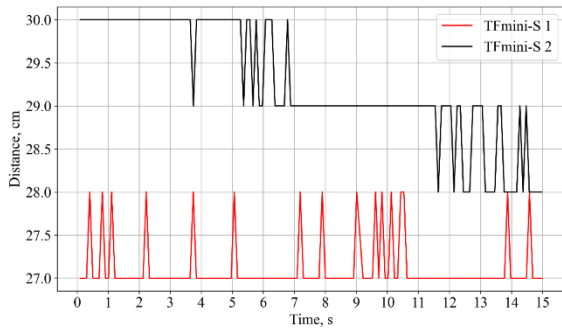


Figure 16: Comparison of two TFmini-S units at 30 cm.

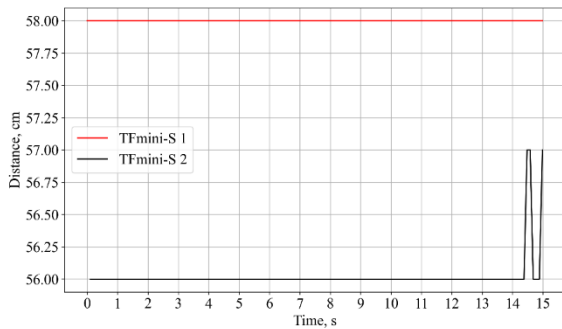


Figure 17: Comparison of two TFmini-S units at 60 cm.

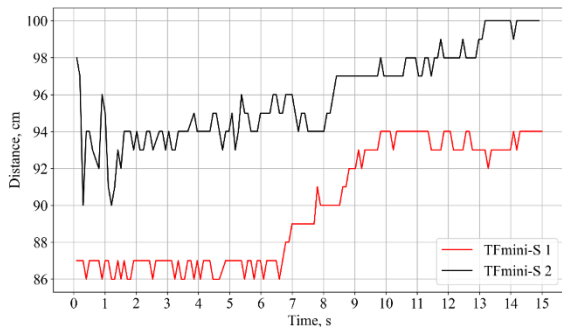


Figure 18: Comparison of two TFmini-S units at 100 cm.

Table 5: Average distance readings for each HC-SR04-P unit.

Test Distance, cm	Average readings, cm	
	TFmini-S 1	TFmini-S 2
5	1.67	3.18
30	27.12	29.15
60	58.00	56.08
100	90.30	96.25
RMSE, cm	5.42	2.89

Results, shown in Table 5, indicate that the TFmini-S exhibits larger deviations at all tested distances compared to HC-SR04 and HC-SR04-P sensors.

The Root Mean Square Errors for individual TFmini-S sensors are 5.42 cm and 2.89 cm, indicating a notable decrease in accuracy compared to the results from ultrasonic sensors.

Examining its specifications provides a possible explanation. The claimed operating range is 0.1 m to 12 m – three times greater than that of the HC-SR04 and HC-SR04-P. Additionally, its range resolution is 1 cm, which prevents more precise distance readings.

This suggests that the TFmini-S may be more appropriate for applications where extended range is prioritized over fine measurement resolution.

4 ROLLATOR GAIT ANALYSIS

Based on the results of previous tests, the HC-SR04-P appears to be the most suitable sensor for use with the rollator.

To assess the performance of the sensor for use in Machine Learning applications, it is important to evaluate how well it captures data under controlled conditions that simulate human gait.

Therefore, a series of tests imitating a person’s gait will be conducted. Instead of walking with the device, the subject's legs will be positioned at various relative distances to the sensors, installed on the rollator. This approach ensures a controlled and repeatable testing environment, allowing for consistent data collection and more reliable insights into sensor performance.

4.1 Rollator System Setup

Figure 19 illustrates the sensor mounting configuration on the rollator. The sensors are positioned beneath the rollator’s seat and attached to the housing that carries the PCB with the Raspberry Pi Zero W, auxiliary sensors, and the Jetson Nano 2 GB.



Figure 19: Prototype Rollator Integration of Sensors and Processing Hardware.

The Raspberry Pi is responsible for collecting data from all connected sensors and transmitting it to the Jetson Nano, which functions as the MQTT broker.

Sensor data is accessed via a laptop that connects to the MQTT broker, and subsequently stored for future analysis.

4.1.1 Nyquist Theorem

Before proceeding with gait tests, it is needed to check whether the sampling rate, in our case the step frequency, satisfies the Nyquist Theorem [17].

If a signal contains frequency components up to a maximum frequency f_{max} , then the minimum sampling rate required to avoid loss of information is:

$$f_s \geq 2f_{max} \quad (2)$$

where f_s is the sampling frequency (or sampling rate).

During previous test with sleep time of 0.1 seconds between cycles, samples were taken with Raspberry Pi Zero at a rate of $f_s = 8.7 \text{ Hz}$, with average sampling period of $T_s = 0.115 \text{ s}$. This implies that, to satisfy the Nyquist Theorem, the maximum step frequency f_{max} would need to be:

$$f_{max} \leq \frac{f_s}{2} = \frac{8.7 \text{ Hz}}{2} = 4.35 \text{ Hz}. \quad (3)$$

This corresponds to a minimum step period of $T_{min} \geq 0.23 \text{ s}$. In other words, to violate the theorem, a single leg would need to step faster than every 0.23 seconds, or make approximately 5 steps per second. The step frequency is estimated to be around 1 step per second, or 1 Hz.

This confirms that the Nyquist Theorem is satisfied and tests can be continued.

4.1.2 HC-SR04-P Maximum Sampling Rate

While still on the subject of sampling rate, it is worth examining the maximum achievable sampling rate of the HC-SR04-P when used with the Raspberry Pi Zero W.

The sampling rate is dependent on the distance from the sensor to the obstacle. For example, if one object is located 5 cm from the sensor and another at 100 cm, the signal's flight time will be 20 times shorter in the first case than in the second. As a result, the sensor can proceed with the next reading much faster in the first scenario, leading to a higher sampling rate.

For the following calculations, HC-SR04-P's maximum specified operating distance of 400 cm will be used as the reference distance.

Knowing the distance to the obstacle, which is 4 m, and speed of sound, which is 343 m/s, maximum time of flight t_{max} can be calculated:

$$t_{max} = \frac{4 \text{ m} \times 2}{343 \text{ m/s}} \approx 23.3 \text{ ms}. \quad (4)$$

The sensor requires a short delay (~1 ms) before a new measurement starts, so assume a minimum cycle time of $t_{max} \approx 24 \text{ ms}$.

Having maximum time of flight t_{max} , maximum theoretical sampling frequency can be found:

$$f_{max} = \frac{1}{0.024 \text{ s}} \approx 41.7 \text{ Hz}. \quad (5)$$

Given that on the rollator two sensors are being used sequentially, the theoretical maximum sampling rate would be:

$$\frac{41.7}{2} \approx 20.8 \text{ Hz}. \quad (6)$$

On practice, maximum sampling rate of $f_{max} = 15.9 \text{ Hz}$ was achieved.

4.1.3 Maximum Sampling Rate with Raspberry Pi

The previous result was achieved using a test script focused solely on collecting data from the ultrasonic sensors. However, in the actual project, the `aktimuwGetData.py` script will be used. This script gathers information from five additional sensors, which increases the runtime of each cycle and consequently reduces the sampling rate.

Using the previously mentioned 400 cm distance to an obstacle and the current script setup with a sleep time of 0.1 seconds between cycles, the sampling rate with `aktimuwGetData.py` is 7.3 Hz.

Referring back to the Nyquist Theorem, it can be observed that the condition is still satisfied.

By minimizing the sleep time between cycles, a maximum sampling rate of 10.3 Hz was achieved.

4.2 Gait Test Methodology

Gait analysis is essential for tracking a person's posture, helping to improve their overall health and well-being [18], [19], especially for elderly [20].

The following test will be conducted as follows (an example is shown in Figure 20):

- Start with the right leg in front and the left leg in the back; hold this position for 5 seconds.
- Move both legs to the middle position; hold for 5 seconds.
- Switch to the right leg in the back and the left leg in front; hold for 5 seconds.
- Repeat the cycle from the beginning.

Test will be repeated with a reduced holding time of 2 seconds per position:

- Start with the right leg in front and the left leg in the back; hold this position for 2 seconds.
- Move both legs to the middle position; hold for 2 seconds.
- Switch to the right leg in the back and the left leg in front; hold for 2 seconds.
- Repeat the cycle for 20 seconds.

The "middle position" refers to a stance in which a straight leg is positioned in front of the rollator, with an approximate distance of 30–35 cm between the leg and the sensors.

The test will be performed with two different distances between the back leg’s knee and the middle position – 30 cm and 15 cm – to simulate larger and smaller steps.



Figure 20: Example of a stance with right leg in the front (the middle position) and the left leg in the back.

Additionally, a moving average filter with a window size of 5 will be applied to produce smoothed results alongside the raw data.

4.3 Results

In Figure 21, the results of the first test are shown. Each stance change – which happens approximately every 5 seconds – is represented by vertical dashed orange line.

The test begins with the left leg positioned back, 30 cm from its knee to the middle position, while the right leg is in the middle position. Around the 5-second mark, the right leg is moved forward to the middle position which is indicated by vertical dashed orange line. At this point, a large spike in the readings is observed, jumping to approximately 200 cm. This is most likely caused by the ultrasonic signal being

reflected off the folds in the fabric of the trousers. Additionally, having the back leg positioned 30 cm behind creates a rather acute angle between the leg and the sensor (Fig.20), further increasing the likelihood of signal reflection and inaccurate readings.

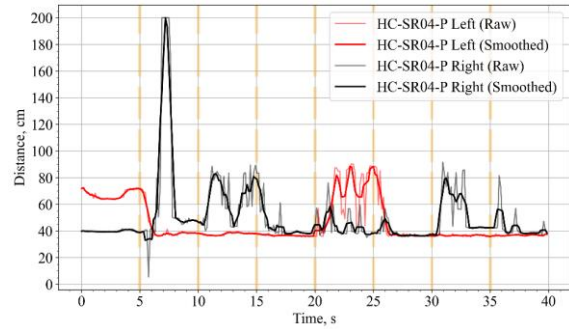


Figure 21: Step test with 30 cm amplitude and 5 s cycle time.

After this spike, the readings stabilize. Around the 10-second mark, the right leg is moved back 30 cm and held in place for 5 seconds. During this phase, a noticeable dip in the distance readings is observed. Following this, the right leg is returned to the middle position, and the cycle is repeated once more.

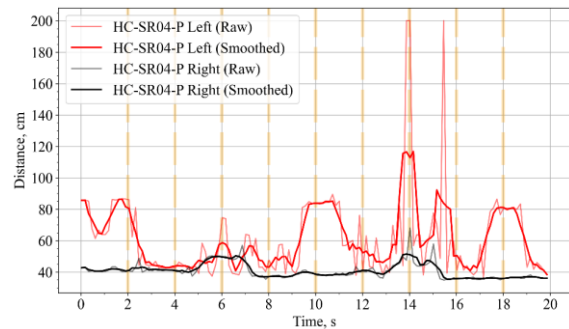


Figure 22: Step test with 30 cm amplitude and 2 s cycle time.

Figure 22 shows similar behavior to the previous test; however, each position is now held for a shorter duration – only 2 seconds. In this test stance change happens every 2 seconds, as shown by vertical dashed orange line.

It is worth noting that, since the holding period is shorter and transitions between positions are not instantaneous, there is an increased potential for confusion in the sensor readings. This is particularly visible between the 12- to 16-second marks.

Additionally, occasional spikes to 200 cm continue to occur, likely due to signal reflections.

Despite these irregularities, the different leg positions are still recognizable in the plot.

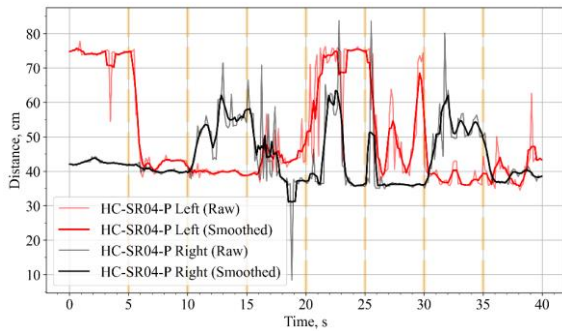


Figure 23: Step test with 15 cm amplitude and 5 s cycle time.

Moving to the next test, Figure 23 displays the results of the run with the back leg positioned with the knee approximately 15 cm behind the middle position, with each stance held for 5 seconds.

Overall, the different positions can be distinguished; however, the back position of the left leg is measured as 35 cm away from the middle, indicating some inaccuracy. On the right leg, the sensor readings are closer to the actual distance between the sensor and the leg.

It is also notable that the spikes up to 200 cm observed in previous tests are now absent. This supports the assumption that reducing the back leg’s distance decreases the angle between the leg and the sensor, thereby lowering the likelihood of signal reflections and missed measurements.

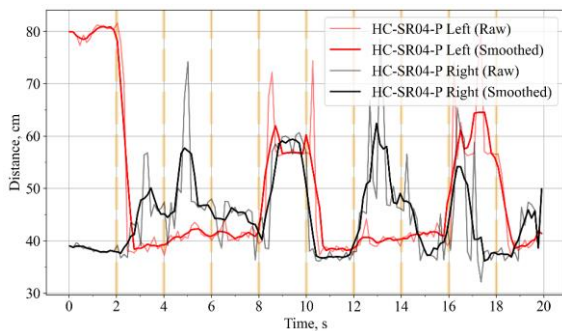


Figure 24: Step test with 15 cm amplitude and 2 s cycle time.

Figure 24 shows the results of a test similar to the previous one, but with each position held for 2 seconds. Distance detection across various stances is once again quite satisfactory, especially considering the potential sources of inaccuracy previously discussed: signal reflections from fabric

folds, the shorter holding time for each position, and the transition period between stances.

Additionally, the slight inaccuracy observed on the left sensor appears to be somewhat reduced in this test. This suggests that the issue is likely not with the sensor itself but rather influenced by external factors.

Overall, the HC-SR04-P sensors demonstrate reliable performance in position and distance detection, though they are not without flaws. However, it is important to consider that the AktiMuW project is intended to assist elderly individuals with mobility, and they are unlikely to take steps larger or faster than those observed during the tests.

Taking this into account – along with the previous analysis of the different sensor types’ performance in the current rollator Raspberry Pi setup, as well as factors like price and reliability – the HC-SR04-P remains the most suitable choice for the AktiMuW project, it gives reliable information for further gait analysis and processing by machine learning algorithms.

5 CONCLUSIONS

After completing all the tests and analyzing the sensors, a decision can be made regarding which sensor should be used.

The HC-SR04 demonstrated very good accuracy with the Root Mean Square Error at 0.64–0.89 cm; however, to use it on the rollator, a new PCB with 5V power traces for the sensors and voltage dividers on the ECHO pin would need to be created.

The HC-SR04 exhibited low Root Mean Square Error values between 0.64 cm and 0.89 cm, indicating a relatively precise measurement capability. However, integrating it into the rollator would require the development of a new PCB with 5V power traces and voltage dividers on the ECHO pin.

The HC-SR04-P resolves the power issue of the HC-SR04, as it can operate directly with 3.3V of Raspberry Pi Zero. It also demonstrated comparable precision, with RMSE values of 0.57 cm and 0.78 cm across two units.

The TFmini-S, a LiDAR-based sensor operating on a different measurement principle, was considered as an alternative. However, test results indicated lower measurement accuracy, with RMSEs of 5.42 cm and 2.89 cm. This reduced precision can be explained by the sensor’s measurement principle and focused measurement spot. Furthermore, it is at least 10 times more expensive and requires 5V power.

The final gait test of the HC-SR04-P on the rollator confirms that the sensors are a suitable solution for the project and further processing by machine learning algorithms to identify leg position, usage and other states of use of rollator.

ACKNOWLEDGEMENTS

This research project underlying this contribution was funded by the Federal Ministry of Education and Research under the grant number FKZ 03WIR3122A. The responsibility for the content of this publication lies with the author.

REFERENCES

- [1] World Health Organization, "Ageing and Health," October 2022, [Online]. Available: <https://www.who.int/news-room/fact-sheets/detail/ageing-and-health>.
- [2] E. Jaul and J. Barron, "Age-Related Diseases and Clinical and Public Health Implications for the 85 Years Old and Over Population," *Front Public Health*, vol. 5, p. 335, 2017.
- [3] V. Kurumbaparambil, S. Rajanayagam and S. Twieg, "Modular Robotic Reinforcement Learning Platform for Object Manipulation," 2024, Universitäts- und Landesbibliothek Sachsen-Anhalt, [Online]. Available: <https://doi.org/10.25673/115703>.
- [4] Translationsregion für digitalisierte Gesundheitsversorgung, "Aktiv im Alter durch Multisensorische Umfeldwahrnehmung – pflege- und versorgungswissenschaftlich evaluative Begleitung der co-kreativen Entwicklung," [Online]. Available: <https://inno-tdg.de/projekte/aktimuw/>.
- [5] F. Mubarak and R. Suomi, "Elderly Forgotten? Digital Exclusion in the Information Age and the Rising Grey Digital Divide," *INQUIRY*, 2022, [Online]. Available: <https://doi.org/10.1177/00469580221096272>.
- [6] S. Twieg and R. Menghani, "Analysis and Implementation of an Efficient Traffic Sign Recognition," in 11th International Conference on Applied Innovations in IT (ICAIIIT), Köthen, 2023.
- [7] Z. Wu, Y. Huang, L. Wang, X. Wang and T. Tan, "A comprehensive study on cross-view gait based human identification with deep cnns," *IEEE transactions on pattern analysis and machine intelligence*, vol. 39, no. 2, 2016.
- [8] E. J. Harris, I. Khoo and E. Demircan, "A Survey of Human Gait-Based Artificial Intelligence Applications," *Front. Robot. AI*, 03 January 2022, Sec. Biomedical Robotics, Volume 8 – 2021, [Online]. Available: <https://doi.org/10.3389/frobt.2021.749274>.
- [9] ElecFreaks.com, "Ultrasonic Ranging Module HC - SR04," [Online]. Available: <https://www.electfreaks.com/download/HC-SR04.pdf>.
- [10] E. Blasch et al., "Machine Learning/Artificial Intelligence for Sensor Data Fusion—Opportunities and Challenges," in *IEEE Aerospace and Electronic Systems Magazine*, vol. 36, no. 7, pp. 80-93, 1 July 2021, [Online]. Available: <https://doi.org/10.1109/MAES.2020.3049030>.
- [11] Y. LeCun, Y. Bengio and G. Hinton, "Deep learning," *Nature*, vol. 521, 2015.
- [12] R. S. Sutton and A. G. Barto, "Reinforcement Learning: An Introduction," *IEEE Transactions on Neural Networks*, vol. 9, no. 5, pp. 1054-1054, 1998, [Online]. Available: <https://doi.org/10.1109/TNN.1998.712192>.
- [13] S. M. Alfayeed and B. S. Saini, "Human Gait Analysis Using Machine Learning: A Review," 2021 International Conference on Computational Intelligence and Knowledge Economy (ICCIKE), Dubai, United Arab Emirates, 2021, pp. 550-554, [Online]. Available: <https://doi.org/10.1109/ICCIKE51210.2021.9410678>.
- [14] Roboter-Bausatz.de, "Datenblatt - HC-SR04-P Ultraschallsensor Entfernungsmesser," [Online]. Available: <https://www.roboterbausatz.de/datasheet/RBS11813.pdf>.
- [15] Benewake (Beijing) Co. Ltd., "Product Manual of TFmini-S," [Online]. Available: <https://en.benewake.com/uploadfiles/2025/04/20250430175136263.pdf>.
- [16] T. O. Hodson, "Root-mean-square error (RMSE) or mean absolute error (MAE): when to use them or not," *Geosci. Model Dev.*, vol. 15, pp. 5481–5487, 2022, [Online]. Available: <https://doi.org/10.5194/gmd-15-5481-2022>.
- [17] C. E. Shannon, "Communication in the Presence of Noise," in *Proceedings of the IRE*, vol. 37, no. 1, pp. 10-21, Jan. 1949, [Online]. Available: <https://doi.org/10.1109/JRPROC.1949.232969>.
- [18] Y. Wahab and N. A. Bakar, "Gait analysis measurement for sport application based on ultrasonic system," 2011 IEEE 15th International Symposium on Consumer Electronics (ISCE), Singapore, 2011, pp. 20-24, [Online]. Available: <https://doi.org/10.1109/ISCE.2011.5973775>.
- [19] R. B. Huitema, A. L. Hof and K. Postema, "Ultrasonic motion analysis system—measurement of temporal and spatial gait parameters," *Journal of Biomechanics*, vol. 35, no. 6, pp. 837-842, 2002, [Online]. Available: [https://doi.org/10.1016/S0021-9290\(02\)00032-5](https://doi.org/10.1016/S0021-9290(02)00032-5).
- [20] A. Macie, T. Matson and A. Schinkel-Ivy, "Age affects the relationships between kinematics and postural stability during gait," *Gait & Posture*, vol. 102, pp. 86-92, 2023, [Online]. Available: <https://doi.org/10.1016/j.gaitpost.2023.03.004>.